Effect of Static Stress on Iron Loss in a Synchronous Reluctance Machine

Deepak Singh, Paavo Rasilo, Floran Martin, Anouar Belahcen and Antero Arkkio

Aalto University, Department of Electrical Engineering and Automation, Finland
Email: deepak.singh@aalto.fi

This study deals with the effect of static stress due to shrink-fitting and centrifugal force on the field computation and the iron losses of the electrical machines. The concept of stress induced magnetic anisotropy has been presented and implemented in a synchronous reluctance machine model. A stress dependent iron-loss model with experimentally determined loss parameters has been implemented as well. The difference in flux density and finally the losses with and without stress dependency has been analyzed.

Index Terms—**Anisotropy, iron-loss, shrink-fitting, stress.**

I. INTRODUCTION

MAGNETIC properties of electrical steels are known to deviate significantly under mechanical stress. The deformation and deviation in the measured BH loop of the electrical steel sheet under stress, is clearly evident from [1], [2], which implies that both the constitutive law (*i.e.* BH curve) and the loss density change with stress [3], [4]. However these effects are almost always neglected when computing for the magnetic field or during post-processing for the losses. Furthermore, the iron parts of the electrical machines are under significant stress due to the shrink-fitting, centrifugal and magnetic forces. Thus, inclusion of the stress dependency in the numerical analysis of the electrical machine is very important to accurately predict the losses. Previously, various studies have included the stress dependency through the material parameters in their models [5]–[7]. However, the inherent material characteristic and the physical phenomenon were not fully represented due to their simplification in coupling either the material parameters or the multi-physics problem. For instance in [5] and [7], the shear component of the stress tensor has been neglected. Moreover, the calculation of iron losses were performed by employing the equivalent von Mises stress.

This study is based on the implementation of the stress induced anisotropy in an otherwise magnetically isotropic material. Only the static stresses arising from the shrink-fit and the centrifugal forces have been considered for analysis. Also the loss coefficients derived from a stress dependent iron-loss model are used in conjunction with the static stress distribution to analyze effect on the losses.

II. METHOD

Magneto-mechanical interaction and dependency have always been difficult to model. Various possible combinations of the magnetization direction, the stress tensor and their interdependencies make the modeling more complex. The modeling approach can be significantly simplified by determining the material magnetic properties in the principal coordinates thereby eliminating the shear component of the stress tensor.

A. Stress Tensor and Principal Co-ordinate

The principal stress component and the rotation angle of the principal coordinate system with respect to XY-coordinate system can be obtained from the stress tensor component as

$$\sigma_{11,22} = \left(\frac{\sigma_{xx} + \sigma_{yy}}{2} \right) \pm \sqrt{ \left(\frac{\sigma_{xx} + \sigma_{yy}}{2} \right)^2 + \tau_{xy}^2 } \quad (1)$$

$$\theta = \frac{1}{2} \tan^{-1} \left(\frac{2\tau_{xy}}{\sigma_{xx} - \sigma_{yy}} \right) \quad (2)$$

where, σ_{xx}, σ_{yy} are the normal stresses and $\tau_{xy} = \tau_{yx}$ are the shear stresses in XY-coordinate system. Similarly, σ_{11} and σ_{22} are the first and second principal stresses respectively. Furthermore, θ is the angle between the XY-coordinate system and the principal coordinate system.

B. Permeability Tensor

The permeability tensor in the principal coordinate system are determined based on the unidirectional measurements (*i.e.* unidirectional field and coaxial stress). The diagonal elements of the permeability tensor is expressed as an analytical or interpolation functions of the principal stresses σ_{11}, σ_{22} and the magnitude of magnetic flux density $|\boldsymbol{B}|$.

$$\mu_{11} = f(|\boldsymbol{B}|, \sigma_{11}) \text{ and } \mu_{22} = f(|\boldsymbol{B}|, \sigma_{22}). \quad (3)$$

Assuming no spatial anisotropy in the principle coordinate,

$$\mu_{12} = \mu_{21} = 0. \quad (4)$$

Once the permeability tensor in the principal coordinate system is obtained, transformation to XY-coordinate is straightforward,

$$\begin{bmatrix} \mu_{xx} & \mu_{xy} \\ \mu_{xy} & \mu_{yy} \end{bmatrix} = \begin{bmatrix} \cos\theta & -\sin\theta \\ \sin\theta & \cos\theta \end{bmatrix} \begin{bmatrix} \mu_{11} & 0 \\ 0 & \mu_{22} \end{bmatrix} \begin{bmatrix} \cos\theta & \sin\theta \\ -\sin\theta & \cos\theta \end{bmatrix}$$
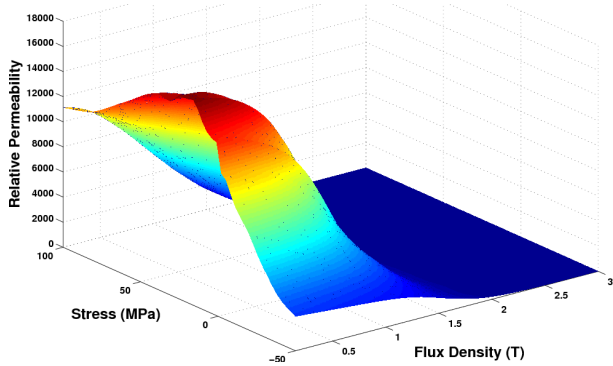
$$(5)$$

Fig. 1. Relative permeability with respect to stress and flux density

Fig. 2. Distribution of difference in flux density (with stress - without stress)

C. Stress Dependent Iron Loss Model

Bertotti's statistical iron losses model [8] is developed for this study, where the hysteresis and excess loss coefficients are stress dependent.

$$p_{\mathrm{v}} = C_{\mathrm{hy}}(\sigma) f \hat{B}^2 + C_{\mathrm{ed}} f^2 \hat{B}^2 + C_{\mathrm{ex}}(\sigma) f^{1.5} \hat{B}^{1.5} \qquad (6)$$

The hysteresis loss coefficient C_{hy} and the excess loss coefficient C_{ex} including their stress dependency, are determined experimentally using a modified Single Sheet Tester (SST) that has a provision of unidirectional stressing. Similarly, the classical eddy-current loss coefficient C_{ed} is calculated analytically (7) as the function of the conductivity λ and the thickness d of the lamination, assuming uniform penetration or distribution of the magnetic flux density along the lamination thickness.

$$C_{\mathrm{ed}} = \frac{\lambda d^2 \pi^2}{6} \qquad (7)$$

Finally, the components of the iron losses are computed as

$$P_{\mathrm{hy}} = \int_{V_{\mathrm{c}}} \left(\sum_{i=1}^{2} \sum_{n=0}^{N} C_{\mathrm{hy}} \left(\sigma_{ii} \right) \left(n\omega_{\mathrm{s}} \right) B_{ii,n}^2 \right) dV \qquad (8)$$

$$P_{\mathrm{ed}} = \int_{V_{\mathrm{c}}} \left(\sum_{i=1}^{2} \sum_{n=0}^{N} C_{\mathrm{ed}} \left(n\omega_{\mathrm{s}} \right)^2 B_{ii,n}^2 \right) dV \qquad (9)$$

$$P_{\mathrm{ex}} = \int_{V_{\mathrm{c}}} \left(\sum_{i=1}^{2} \sum_{n=0}^{N} C_{\mathrm{ex}} \left(\sigma_{ii} \right) \left(n\omega_{\mathrm{s}} \right)^{1.5} B_{ii,n}^{1.5} \right) dV \qquad (10)$$

where, $B_{ii,n}$ is the nth harmonic of the magnetic flux density obtained after projecting the flux density vector $\boldsymbol{B}$ in the principal coordinate. N is the number of harmonics taken into account, ω_{s} is the frequency of the fundamental harmonic.

III. RESULT

A synchronous reluctance machine model was developed using the COMSOL Multiphysic software. The mechanical analysis was done utilizing the plane stress formulation, with a $10\,\mu\mathrm{m}$ of both stator-casing and rotor-shaft shrink-fit. Stress due to centrifugal force of rotation was also included. Once the stress distribution was determined, the method explained in Subsections (II-A) and (II-B) was implemented in stator and rotor iron parts. The s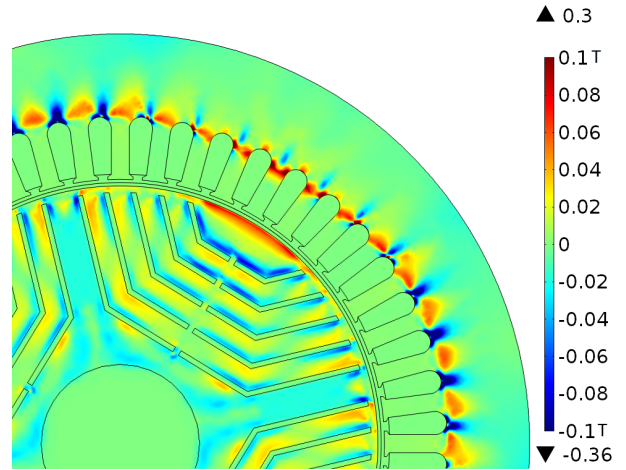tress dependent relative permeability was determined experimentally, as shown in Fig. 1, and used as the constitutive relation. Fig. 2 shows the distribution of the difference in the flux density (i.e. with stress dependency minus without stress dependency), in one of the stationary conditions supplied with a constant current source.

IV. DISCUSSION AND CONCLUSION

From Fig. 2, significant difference in the flux density due to material deterioration under stress, can be observed. In the rotor, the variation is prominent at the iron parts between the flux barrier slits. Additionally, in the stator the difference can be observed at the base of the stator teeth and at the top of the winding slots. Further evaluation of the stress effect on losses along with the SST measurements to determine the stress dependent iron loss model parameters (explained in Subsection II-C) will be presented in the future full paper. Similarly, the difference comparison as well as various levels of stress dependency will also be investigated, i.e. stress dependent relative permeability and/or stress dependent loss model.

REFERENCES

[1] M. LoBue, C. Sasso, V. Basso, F. Fiorillo, and G. Bertotti, "Power losses and magnetization process in fesi non-oriented steels under tensile and compressive stress," *Journal of Magnetism and Magnetic Materials*, vol. 215216, no. 0, pp. 124–126, 2000.
[2] D. Miyagi, K. Miki, M. Nakano, and N. Takahashi, "Influence of compressive stress on magnetic properties of laminated electrical steel sheets," *IEEE Transactions on Magnetics*, vol. 46, pp. 318–321, Feb 2010.
[3] Y. Kai, Y. Tsuchida, T. Todaka, and M. Enokizono, "Influence of stress on vector magnetic property under alternating magnetic flux conditions," *IEEE Transactions on Magnetics*, vol. 47, pp. 4344–4347, Oct 2011.
[4] Y. Kai, Y. Tsuchida, T. Todaka, and M. Enokizono, "Influence of stress on vector magnetic property under rotating magnetic flux conditions," *IEEE Transactions on Magnetics*, vol. 48, pp. 1421–1424, April 2012.
[5] N. Takahashi and D. Miyagi, "Effect of stress on iron loss of motor core," in *Electric Machines Drives Conference (IEMDC), 2011 IEEE International*, pp. 469–474, May 2011.
[6] K. Fujisaki and S. Satoh, "Numerical calculations of electromagnetic fields in silicon steel under mechanical stress," *IEEE Transactions on Magnetics*, vol. 40, pp. 1820–1825, July 2004.
[7] D. Miyagi, N. Maeda, Y. Ozeki, K. Miki, and N. Takahashi, "Estimation of iron loss in motor core with shrink fitting using fem analysis," *IEEE Transactions on Magnetics*, vol. 45, pp. 1704–1707, March 2009.
[8] G. Bertotti, "General properties of power losses in soft ferromagnetic materials," *IEEE Transactions on Magnetics*, vol. 24, pp. 621–630, Jan 1988.